HOW MANY EXTENSIONAL STAGES MARKED THE VARISCAN GRAVITATIONAL COLLAPSE IN THE BOHEMIAN MASSIF?

Ondřej Bárta [1*], Rostislav Melichar [1] & Jan Černý [2]

[1] *Department of Geological Sciences, Faculty of Science, Masaryk University, Kotlářská 2, 611 37 Brno, Czech Republic, e-mails: 211447@mail.muni.cz, melda@sci.muni.cz*
[2] *Institute of Geology, Czech Academy of Sciences, 165 00 Praha 6, Czech Republic, e-mail: jcerny@gli.cas.cz*
** Corresponding author*

Bárta, O., Melichar, R. & Černý, J., 2021. How many extensional stages marked the Variscan gravitational collapse in the Bohemian Massif? *Annales Societatis Geologorum Poloniae,* 91: 121–136.

Abstract: Tectonic development of the Variscan belt in Central Europe included, besides important compression, also an extensional phase related to gravitational collapse, which governed the origin of many sedimentary basins and magmatic bodies. One of these bodies is the Benešov pluton, featuring primary magmatic fabrics as well as deformational fabrics, related to subsequent extensional stages. Recognition of these fabrics and their links to other significant extension-induced structures in the Bohemicum and Moldanubicum not only sheds new light on the pluton itself but also extends a general knowledge of deformational stages, accompanying gravitational collapse of the Variscan orogen. The authors found that this pluton was strongly strained in a normal-faulting regime under brittle-ductile conditions. The age of deformation is constrained by a magmatic age of 347 ±3 Ma and by the age of Carboniferous sedimentary cover. New data indicate a three-stage extensional history during the phase of gravitational collapse: (1) Tournaisian extension (~350–345 Ma) within arc-related tonalitic intrusions; (2) late Viséan to Serpukhovian extension (~332–320 Ma), connected to the brittle-ductile unroofing and origin of a NE–SW basin system; and (3) Gzhelian to Cisuralian extension (~303–280 Ma), related to normal faulting and sedimentation in "Permo–Carboniferous" troughs, elongated NNE–SSW. Consequently, the gravitational collapse studied involved a complex succession of individual extensional stages, rather than a simple process.

Key words: Gravitational collapse, anisotropy of magnetic susceptibility, U-Pb zircon geochronology, Variscan orogen, Central Bohemian plutonic complex.

Manuscript received 15 December 2020, accepted 23 March 2021

INTRODUCTION

A collision between Laurussia, Gondwana, and intervening microplates during the Devonian (Edel *et al*., 2018) led to the origin of a large orogenic belt and eventually to the abnormal thickening of the continental crust throughout the Northern Hemisphere (Matte, 1991, 2001; Franke, 1992; Stampfli *et al*., 2002). Subsequent heating of orogenic roots and gravitational instability of the thickened lithosphere dominated during the late orogenic processes (Rey *et al*., 2001; Jadamec *et al*., 2007). The unstable continental lithosphere was subjected to gravitational collapse and a compressional regime was replaced by extension, manifested in large intrusions of granitoids at deep levels and the formation of sedimentary basins at the surface (Malavieille *et al*., 1990; Pešek, 1994; Mazur and Kryza, 1996; Rodríguez-Méndez *et al*., 2016). Variscan geodynamic evolution of Central Europe was characterized by the rapid exhumation of metamorphic rocks during the extensional stages (Pešek, 1994; Lobkowicz *et al*., 1996; Mlynář and Melichar, 1999; Klomínský *et al*., 2010; Žák *et al*., 2012, 2017; Kroner and Romer, 2013). This exhumation was controlled mainly by lithospheric extension and gravitational forces (Henk, 1996), and late Palaeozoic sedimentary basins originated in the Variscan mountains during this process (Malavieille *et al*., 1990). The findings of the present authors suggest that among the best places to study the extensional history of the Variscan orogen are upper Palaeozoic intrusions, such as the Benešov pluton. Since its first description (Koutek and Urban, 1929), it has been known under the name "older biotite granite". Owing to the high degree of deformation, the rocks were considered to be of a very old age, i.e., older than other Variscan plutons nearby (Svoboda, 1964, Holub *et al*., 1997a, b). Orlov (1933) was the only one, who considered it to be younger, owing to the fact that the Benešov pluton was slightly more acidic than other Variscan plutonic rocks in the vicinity. In spite of the large volume of data obtained to date from the Variscan orogen, information provided by the Benešov pluton sheds new light on the late-orogenic evolution of the Variscides and the tectonic setting for the emplacement of the abundant granitoid intrusions. This paper provides new data on the age of the Benešov pluton and its subsequent deformation, placing them in the wider geodynamic context of late-Variscan extension.

REGIONAL SETTING

The study area lies in the central part of the Bohemian Massif, where two large terranes, i.e., the Bohemicum and the Moldanubicum, are next to each other (Fig. 1). The Moldanubicum represents an exhumed orogenic root of the Variscan Belt (e.g., Schulmann *et al*., 2009), formed by rocks metamorphosed under granulite/eclogite to amphibolite facies, while the Bohemicum forms the highest part of the basement in the Variscan orogen (Franke, 2000). This is evidenced by its uppermost part – the Barrandian area with unmetamorphosed Neoproterozoic to lower Palaeozoic

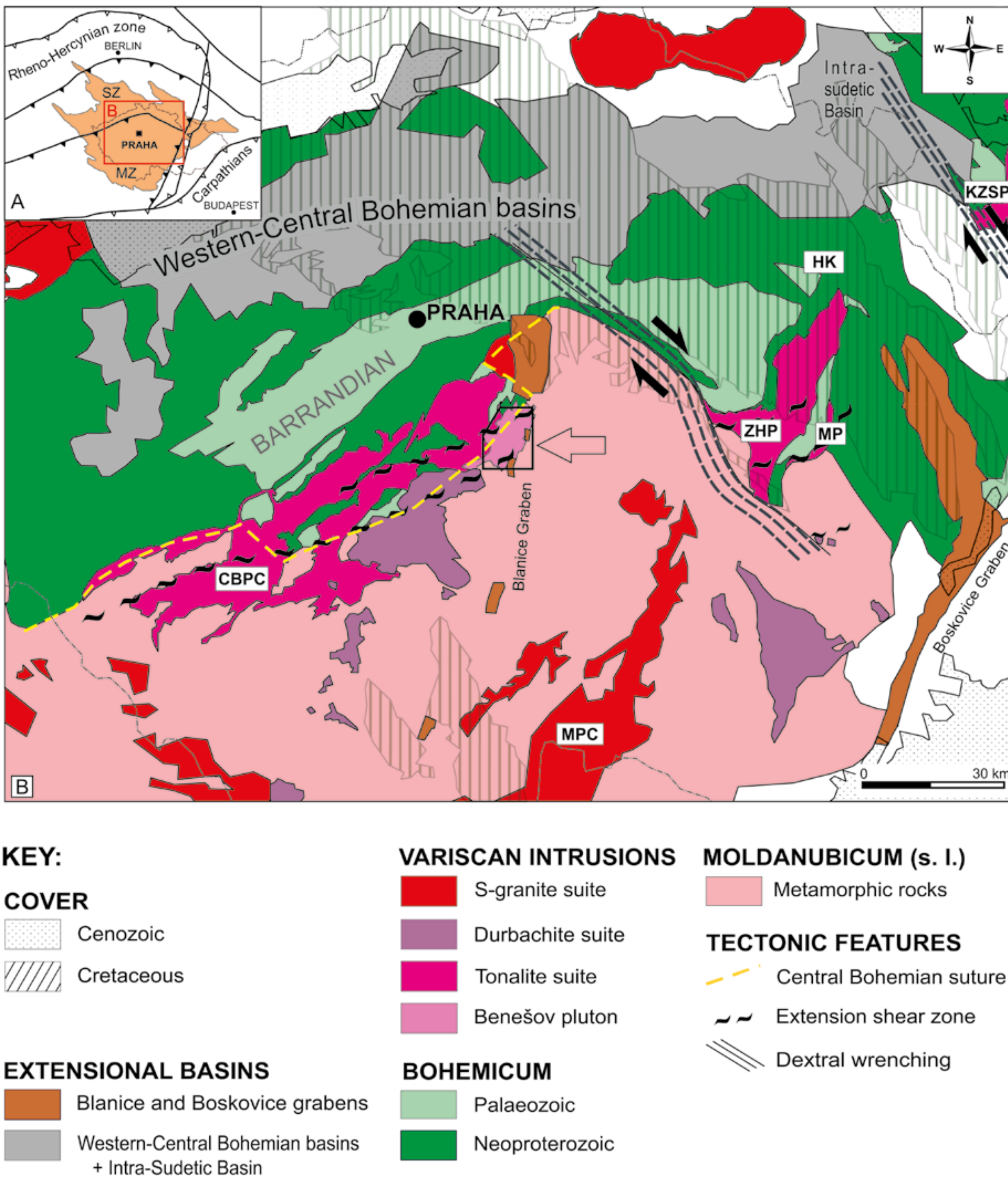

Fig. 1. Location of the study area within the Central European Variscan Belt (**A**) and the Bohemian Massif (**B**); after Melichar (2004), simplified. Explanations: CBPC – Central Bohemian plutonic complex, HK – Hradec Králové, KZSP – Kłodzko-Złoty Stok pluton, MP – Miřetín pluton; MZ – Moldanubian zone; SZ – Saxothuringian zone, ZHP – Železné hory plutonic complex.

sedimentary rocks. The Bohemicum/Moldanubicum boundary is overprinted by the Central Bohemian shear zone and intruded by plutonic rocks of the Central Bohemian plutonic complex (CBPC). Its original elongation NE–SW to N–S was altered to a zig-zag shape by younger, dextral wrenching in Serpukhovian to Bashkirian time (Edel *et al*., 2018).

The Bohemian Massif was intruded by three main Permo-Carboniferous plutonic suites, accompanied by a large number of secondary ones (Klomínský *et al*., 2010): (1) the tonalite suite emplaced into the Central Bohemian shear zone, forming the main part of the CBPC. The suite contains mainly Tournaisian (354–346 Ma) arc-related, calc-alkaline granitoids (Vejnar, 1974; Holub *et al*., 1997b; Janoušek *et al*., 2000; Janoušek and Gerdes, 2003; Dragoun *et al*., 2009). Equivalent rocks are exposed also in the Železné hory plutonic complex (Verner and Vondrovic, 2010) and the Kłodzko-Złoty Stok pluton (Klomínský *et al*., 2010; Mikulski *et al*., 2013; Jokubauskas *et al*., 2018); (2) the durbachite suite, consisting of the Viséan (343–332 Ma) ultrapotassic intrusions of quartz melasyenite, independently attached to the tonalite plutonic complex in central Bohemia. This suite is widespread in the Moldanubicum (Klomínský *et al*., 2010) and variously deformed (Mlynář and Melichar, 1999); and (3) the S-granite suite with a broad time range of its origin (320–290 Ma). It forms the Moldanubian plutonic complex in the central part of the Moldanubicum and several bodies on the NW and NE periphery of the Bohemian Massif (Klomínský *et al*., 2010).

A comparison of the sedimentary-basin elongations and the geometries of deformational fabrics in the magmatic intrusions revealed causal relationships between the processes of their formation (e.g., Malavieille, 1993). The oldest extensional sedimentary basins (Famennian–Tournaisian; i.e., ~370 to ~345 Ma) are the Świebodzice Basin in the Polish Sudetes (Porębski, 1981, 1990) and those concealed beneath Cretaceous sediments, near Hradec Králové (Chlupáč and Zikmundová, 1976; Čech *et al*., 1989). The origin of the Intra-Sudetic Basin is dated as middle to early late Viséan (~335 Ma; Turnau *et al*., 2002). The Intra-Sudetic Basin was incorporated more recently into a younger (mainly Moscovian–late Cisuralian, i.e., ~311 to ~276 Ma), intracontinental basin system in the western, central and northern parts of the Bohemian Massif, which is elongated NE–SW (Pešek, 1994). Late Variscan sedimentation in the troughs, elongated NNE–SSW to N–S, took place from the Gzhelian (~303 Ma) to the late Cisuralian (~280 Ma; Falke, 1975). One of these youngest troughs is the Blanice Graben (also referred to as the Blanice "Furrow"), the sedimentary fill of which covers the study area of the Benešov granodiorite in several places.

METHODS

Geologic structures were studied on a mesoscopic scale at 32 sites and in thin sections from the most representative localities (10). The thin sections were made from oriented samples to keep track of the original orientation of structures in the field, especially the sense of shear in asymmetric structures. The geometry of a strain ellipsoid with axes $X \geq Y \geq Z$ was characterized by its anisotropy $Pg = X / Z$ and by the geometrical shape parameter $Tg = (2Y - X - Z) / (X - Z)$. If Tg is negative (i.e., $-1 \leq Tg < 0$), the strain ellipsoid is prolate, otherwise (i.e., $0 < Tg \leq +1$) it is oblate.

Anisotropy of magnetic susceptibility

The anisotropy of magnetic susceptibility (AMS) was studied together with mesoscopic structural measurements at 33 sites. The AMS was used for the study of the preferred orientation of magnetic minerals in rocks (Graham, 1954; Borradaile and Henry, 1997), particularly in granites (Bouchez *et al*., 1990; Bouchez, 1997, 2000; Hrouda, 1999). Magnetic susceptibility can be visualized as an ellipsoid with three principal axes, usually with different lengths ($k_1 \geq k_2 \geq k_3$; Tarling and Hrouda, 1993). The maximum axis represents the magnetic lineation, while the minimum one is perpendicular to the magnetic foliation. The geometry of the AMS ellipsoid can be described by three independent parameters, i.e., bulk susceptibility $k_{mean} = (k_1 + k_2 + k_3) / 3$, the degree of anisotropy $P = k_1 / k_3$ (Nagata, 1961), and the shape parameter $T = 2\ln(k_2 / k_3) / \ln(k_1 / k_3) - 1$ determining prolate ($-1 \leq T < 0$) or oblate ($0 < T \leq 1$) geometries (Jelínek, 1981).

More than 450 oriented samples were taken, using a portable drill at 33 sampling sites, distributed across the entire study area. The AMS data were obtained, using KLY-3s Kappabridge (Jelínek and Pokorný, 1997) and statistically analysed by Anisoft software (Chadima and Jelínek, 2008). The contribution of individual minerals to the overall magnetic susceptibility was analysed on finely powdered specimens, using a CS-4 furnace and KLY-4S Kappabridge (Hrouda, 1994; Jelínek and Pokorný, 1997). The acquired data were plotted in Cureval software (version 8.0.2). The samples were heated from room temperature to 700 °C and cooled back to room temperature in an argon environment.

Zircon U–Pb dating

The radiometric age of the Benešov granodiorite was determined in zonal zircon grains by laser ablation inductively coupled plasma mass spectrometry (LA ICP-MS) at the Laboratory of Geological Processes, Institute of Geology, Czech Academy of Sciences, Prague. The isotopic ratios $^{207}Pb/^{235}U$ and $^{206}Pb/^{238}U$ were acquired by means of an Element 2 high-resolution sector field mass spectrometer (Thermo Fisher Scientific), coupled with a 193 nm ArF Analyte Excite excimer laser ablation system (Teledyne/Cetac). The helium carrier gas was flushed through the two-volume ablation cell at a flow rate of 0.7 L/min and mixed with 0.66 L/min Ar and 0.004 L/min N before introduction into the mass spectrometer. The laser was fired at a repetition rate of 5 Hz and fluence of c. 3.5 J/cm^2, using a 22-micron spot size. The acquisitions for all standards and measured samples consisted of a 35-second measurement of a blank followed by the measurement of U and Pb signals from the ablated zircon for another 35 s. The in-house glass-signal homogenizer, with design inspired by Tunheng and Hirata (2004), was used for mixing all the gases and aerosol resulting in a smooth, spike-free signal. The signal was tuned for the maximum sensitivity of Pb and U.

A total of 420 mass scans data was acquired in time-resolved peak-jumping, pulse-counting analogue mode with one point measured per mass peak for ^{206}Pb, ^{207}Pb, ^{235}U, and ^{238}U. Raw data reduction and age calculations, including corrections for baseline, instrumental drift, mass bias, and down-hole fractionation, were carried out, using the Iolite program (v. 3.32; Paton *et al*., 2011) with the VizualAge utility (Petrus and Kamber, 2012). Residual elemental fractionation and instrumental mass bias were corrected by normalization of the internal natural zircon reference material from the Plešovice Quarry (Sláma *et al*., 2008). Zircon reference materials, marked as GJ-1 (Jackson *et al*., 2004; Kylander-Clark *et al*., 2013; Schaltegger *et al*., 2015) and 91500 (Wiedenbeck *et al*., 1995), were analysed periodically during measurement for quality control of resulting data. The zircon U–Pb ages are presented as concordia plots, generated with the Iolite program (Paton *et al*., 2011).

The average Th/U ratio in zircons was used to discriminate whether the obtained data correspond to magmatic or metamorphic crystallization. The values under 0.1 are typical of metamorphic growth (Hoskin and Schaltegger, 2003), while values higher than 0.5 indicate a magmatic origin (Pystina and Pystin, 2019).

RESULTS

Petrography and deformational fabrics

The Benešov pluton is composed mainly of medium-grained porphyritic biotite granodiorite, intruded by a swarm of aplitic dikes. The granodiorite consists mainly of plagioclase, quartz, biotite, a small amount of K-feldspar, and accessory zircon. The typical grain size is 1–3 mm; plagioclase phenocrysts are approximately 10 mm long. A subordinate population of feldspar phenocrysts reaches a size of up to 3 cm (Fig. 2C).

The pluton is limited by a young fault in the north, whereas its western contact is intrusive. The host rock surrounding the pluton in the south and east is Moldanubian biotitic stromatite migmatite with locally developed, ptygmatic folds deforming leucosome veins (Fig. 2A). The contact with the migmatite is sharp and straight (Fig. 2B), parallel to, or cutting the stromatite fabric of the migmatite, flat and steep in outcrops and irregular on the mesoscopic scale. Angular xenoliths of the host rock were observed in the granodiorite near the eastern endocontact of the pluton (Fig. 2F). Unlike the migmatite xenoliths, isolated mafic enclaves formed by diorite rock are rounded and ellipsoidal. The granodiorite rock is cut by numerous aplitic dikes (Fig. 2D), concentrated in the central part of the pluton but also present at its peripheries. These dikes consist of aplitic microgranite with occasional spheroidal tourmaline pods with whitened rims. The aplitic dikes contain granodioritic xenoliths of angular, platy forms (Fig. 2E).

The igneous features of the granodiorite are mostly overprinted by strongly developed brittle-ductile strain fabric. At a mesoscopic scale, a well-developed deformation fabric is defined by a strong foliation and lineation. Two main petrofabrics can be distinguished in the Benešov granodiorite (Fig. 3): (1) fabric A_{meso} striking NNW–SSE to NNE–SSW and steeply dipping mainly to the W, but locally to the E (Fig. 3A). The associated lineation is variable in its trend, plunging mostly WNW at intermediate angles (Fig. 3B); (2) fabric B_{meso} being the dominant mesoscopic foliation, dipping mainly NW at low to medium angles (Fig. 3A). Lineation of fabric B_{meso} is unified, plunging NNW at 10–30° (Fig. 3B). Aplitic dike sheets are usually oriented parallel to the main deformational foliation (Fig. 2D), and sometimes strongly strained as indicated by elongated quartz grains (see Fig. 4A, B) and tourmaline pods (Fig. 4C). These pods are prolate with a shape parameter equal to −0.74 and an anisotropy of 6.85. Mafic magmatic enclaves reveal a similar prolate geometry (Fig. 4D), usually with higher anisotropy (up to ~10–15), but owing to the originally ellipsoidal shape and non-abundant amounts of enclaves, this value should be taken as an approximation.

Microscopically, plagioclase grains show oscillatory zoning (Fig. 5A), especially in the case of euhedral phenocrysts. Plagioclase grains are twinned. Magmatic twinning is typical for phenocrysts, and almost all grains, especially the larger ones, are twinned by subsequent deformation (Fig. 5B). Deformation twins are fine, multiple, and incoherent. Brittle fractures in plagioclase are locally filled with remobilized quartz (Fig. 5C). Some plagioclase grains are affected by sericitization. K-feldspar is present in small amounts; myrmekite structures were also observed. Grains of quartz 0,3–1 mm in size are moderately elongated and characterized by lobate forms, resulting from primary recrystallization (Fig. 5A–C). These grains are divided into sub-grains by the recovery process, which is manifested by undulatory extinction in thin sections under cross-polarized light. Strained quartz grains in some cases are surrounded by fine-grained, recrystallized quartz (Fig. 5E). Flakes of biotite are straight or bent and, in this case, they are concentrated into more-or-less parallel bands and in places associated with muscovite (Fig. 5E, F); chloritization of such biotite was often observed (Fig. 5D, E).

A tectonic overprint of igneous structures is indicated by wavy biotite aggregates and rounded, flattened, and/or crushed mineral grains (Fig. 5F). Strongly foliated rocks may contain newly crystallized phyllosilicates, e.g., muscovite and chlorite (Fig. 5D–F). Simple shear deformation is documented by asymmetric structures, such as σ-porphyroclast systems and/or S-C structures (Fig. 5F), and discrete shear bands in the granodiorite. The sense of the shear indicated by the S-C structure associated with dominant petrofabric B_{meso} indicates normal faulting to the NNW (Fig. 5F); however, sporadic reverse kinematics, approximately in the same direction, was observed.

Magnetic minerals and AMS fabrics

To properly interpret the recognized AMS fabrics, the authors studied the temperature dependence of magnetic susceptibility to determine the main carrier(s) of magnetic susceptibility (MS). The results showed a low k_{mean} value in the order of magnitude of 10^{-4} SI at the beginning of the analysis. Magnetic susceptibility was decreasing continuously

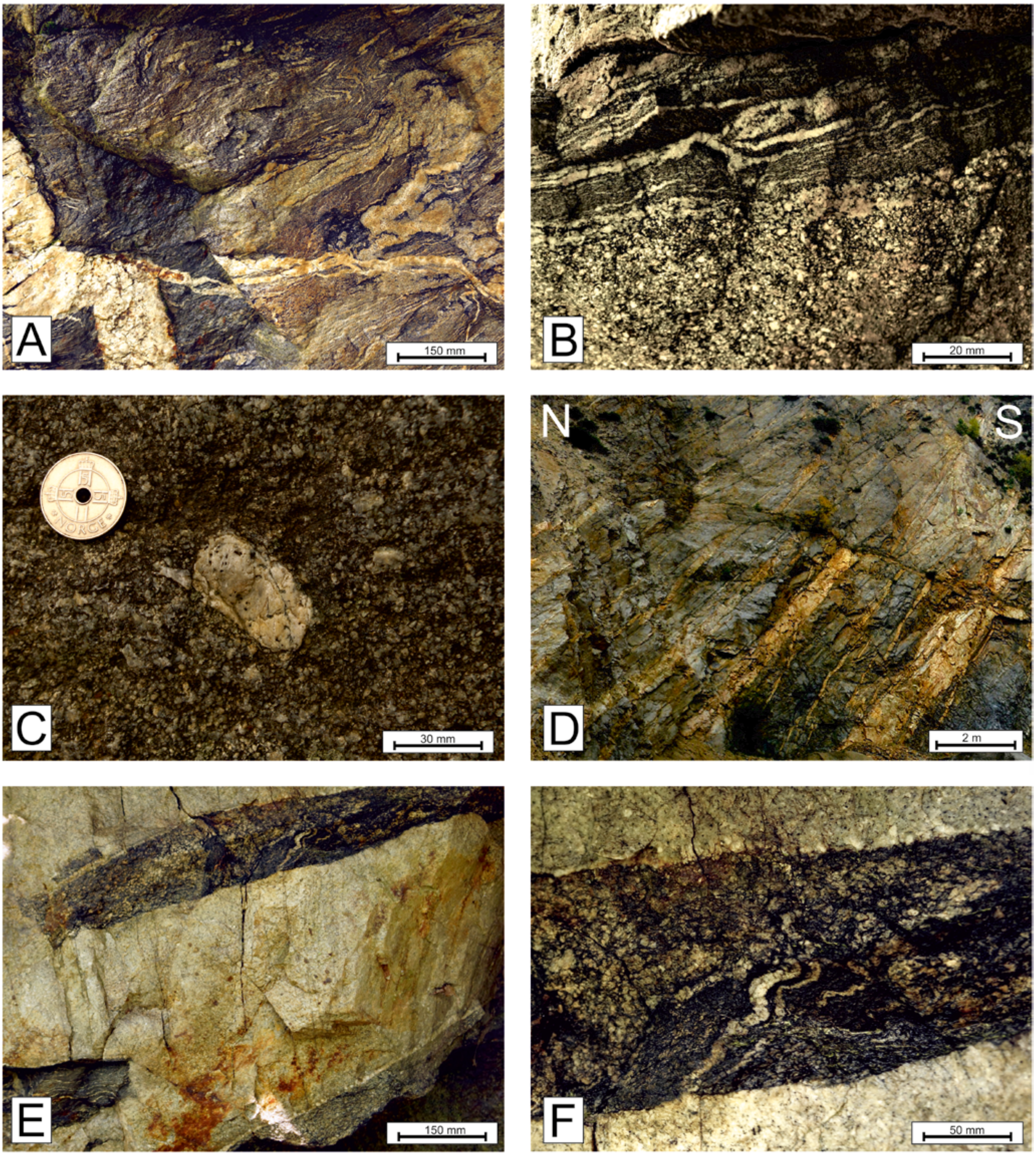

Fig. 2. Mesoscopic structures in the Benešov granodiorite and associated rocks. **A.** Folded Moldanubian migmatite with an aplitic dike (host rock of the Benešov granodiorite), Lhotka Veselka. **B.** A sharp magmatic contact of the Moldanubian migmatite and the Benešov granodiorite, Lhotka Veselka. **C.** Typical Benešov granodiorite with small phenocrysts and a rare large one, Bílkovice Quarry. **D.** Widespread aplitic dikes oriented in a foliation-parallel position, Bílkovice Quarry. **E.** An aplitic dike with platy xenoliths of the Benešov granodiorite, Lhotka Veselka. **F.** An angular migmatite xenolith in the Benešov granodiorite (a close-up view from image E).

with an increasing temperature up to ~200–250 °C. This indicates that the main carriers of the AMS were paramagnetic mineral phases, such as biotite and/or amphibole at the beginning of the analysis. The sudden change in the trend of the curve and initiation of MS increase above ~200 °C indicates newly formed magnetite with a Curie temperature of 585 °C. A small peak at 300 °C indicates a small amount of titanomagnetite, titanomaghemite, and/or pyrrhotite that were also produced by heating, as new magnetic minerals originated during the analysis. These ferromagnetic phases originated mainly during laboratory heating and could not affect the measured AMS fabric under low-temperature

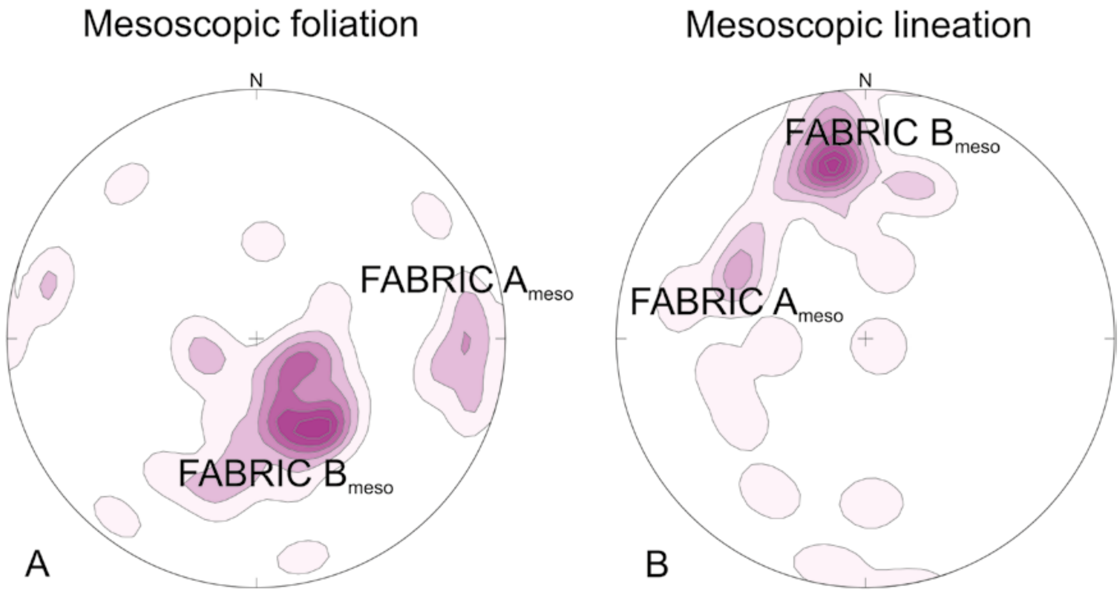

Fig. 3. Orientation of the main mesoscopic foliation (**A**) and lineation (**B**) from the Benešov granodiorite. Equal-area azimuthal projection on the lower hemisphere, number of data: 50 and 30 respectively.

conditions. The thermomagnetic curves exhibit hyperbolic shapes in the range of 0–200 °C (Fig. 6). Thus, the main magnetic carriers responsible for AMS fabrics were paramagnetic minerals.

The AMS results (Fig. 7) showed that the shape parameter T varies from medium prolate to strongly oblate shapes ($-0.483 \leq T \leq +0.777$). The anisotropy degree P indicated anisotropies ranging from 3.3% to 13.2% (P = 1.033––1.132.). Owing to the absence of ferromagnetic phases, the mean magnetic susceptibilities of measured samples were lower (k_{mean} = 0.67 to 4.08 $\times 10^{-4}$ SI) compared to those of other common granites. Based on directional analyses, site affinities, and clustering in the Jelínek diagrams, the authors separated 3 main AMS fabric types in the Benešov granodiorite (Fig. 7): (1) fabric type A_{mag} is represented by sites with a N–S-oriented, subvertical, magnetic-foliation-bearing, W–E to SW–NE-trending, magnetic lineation ($\mathbf{k}_1$), and characterised by the highest anisotropies (10% on average); (2) fabric type B_{mag} involves only sites with gently inclined magnetic foliation and lineation $\mathbf{k}_1$ plunging to the N (7% anisotropy on average); (3) fabric type C_{mag} is linked to steep to vertical magnetic foliation, striking W–E to SW–NE, and vertical magnetic lineation $\mathbf{k}_1$. The average anisotropy is ~5% in this case. This fabric type is sporadically distributed over the entire Benešov granodiorite body.

Although all three fabric types were identified over a large part of the study area, fabric A_{mag} dominates the south-eastern marginal zone of the Benešov pluton near the outcrops of Permian rocks in the Blanice Graben, while fabric B_{mag} is distributed over the whole pluton, and fabric C_{mag} appears sporadically, rather in the central part of the Benešov pluton (Fig. 8).

Zircon U-Pb dating

Zircon grains were separated from granodiorite of the Bílkovice Quarry. Altogether 33 grains with magmatic zoning were used for the radiometric analyses (Tab. 1). Prismatic zircon grains used for this purpose are euhedral and oscillatory-zoned (Fig. 9). The individual U-Pb zircon ages are spread in the range of 340–356 Ma (Tab. 1). Zircon grains yielded concordant U–Pb ages with a mean of 347 ±3 Ma (Fig. 10). The average Th/U ratio in zircons from the Benešov granodiorite equals 0.58 ±0.15, evidencing that the acquired age corresponds to the time of magmatic crystallization.

DISCUSSION

Origin of the pluton and its age

The magmatic origin of the Benešov granodiorite is in accordance with the observations of plagioclase and dated prismatic zircon grains by the authors. These are euhedral and oscillatory-zoned (Figs 5A, 9); as such, they have typical features directly indicating crystallization from a granitoid melt (Shore and Fowler, 1996). The intrusive origin of the rock also is validated by angular xenoliths with contacts parallel to, or cutting, stromatite structure of the migmatite. Sharp and straight contacts between granodiorite and host rocks (Fig. 2B) as well as the xenoliths (Fig. 2F) indicate the stoping process as the main emplacement mechanism of the pluton. The newly acquired radiometric age of 347±3 Ma, obtained on zircons with the high U/Th ratio typical of magmatic origin, define the time of emplacement for the Benešov pluton. The age and petrology of the latter place it within the tonalite suite of the CBPC.

Recorded history in AMS fabrics and mesoscopic structures

Structural analysis of the mesoscopic fabrics revealed the presence of two main petrofabrics (A and B, Fig. 3), which overlap and have their equivalents in AMS fabrics

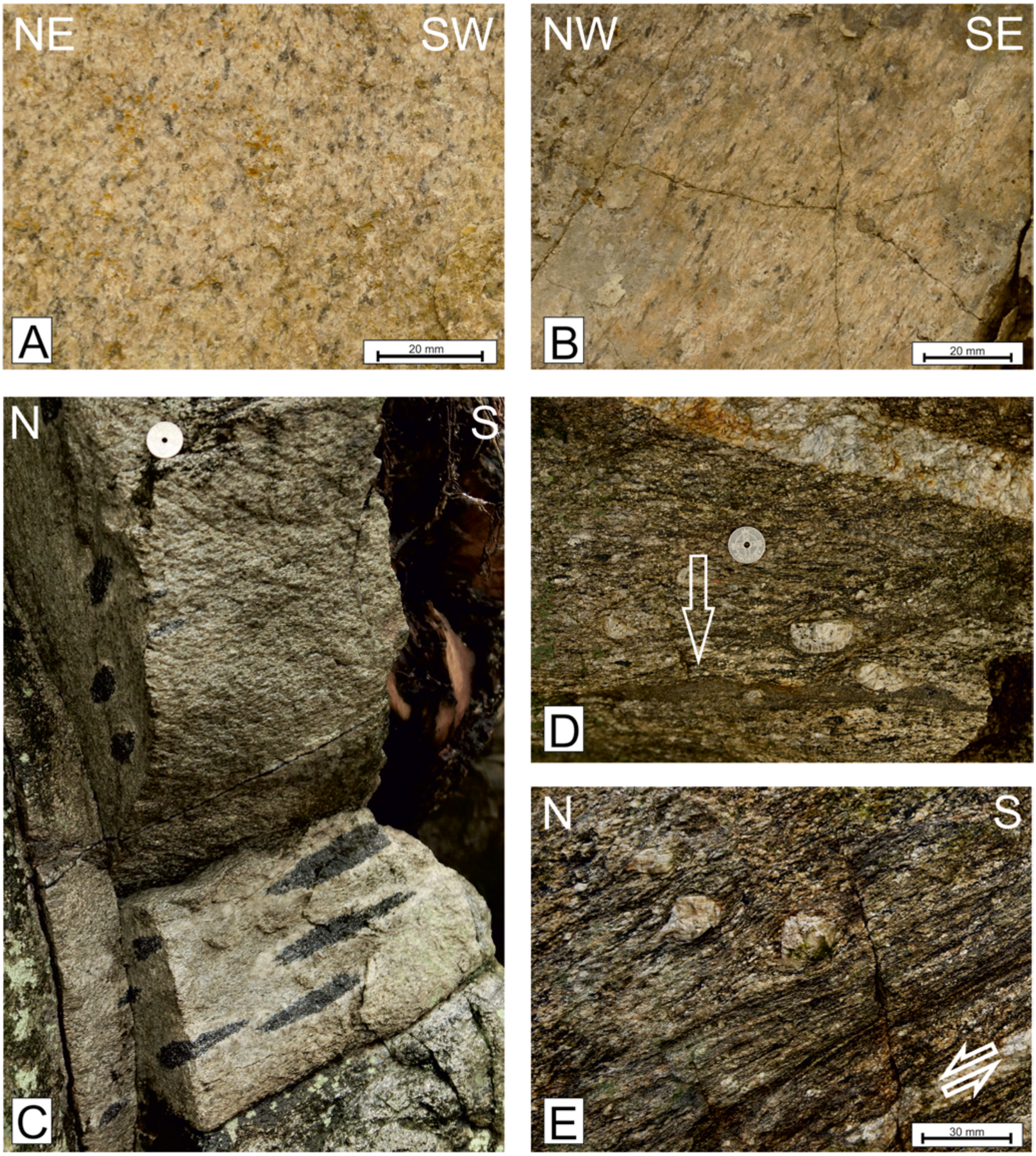

Fig. 4. Mesoscopic strain structures in the Benešov pluton. **A**, **B.** A deformed aplitic dike with prolate geometry of quartz grains in cross-section *XY* (A) and *XZ* (B), Bílkovice Quarry. **C.** Strained tourmaline pods with prolate geometry (see different cross sections), Takonín. **D.** Extreme elongation of a strained mafic enclave, note the almost parallel orientation of all structures, Postupice. **E.** σ-porphyroclast systems with a top-to-the-N sense of movement in the Benešov granodiorite, Postupice.

(Fig. 7). Complementary studies of magnetic fabrics across the entire area revealed three main fabric groups with different structural affinities. Combining both types of observations, the authors can distinguish the following fabrics:

(A) The first group of AMS fabrics (fabric A_{mag}) can be associated with mesoscopic fabric A_{meso}. It includes a steep foliation, striking N–S and plunging to the W or E (Fig. 3). Fabric A is oriented parallel to the Blanice Graben (see Fig. 1) that was formed at ~303–280 Ma (Gzhelian to Cisuralian). This spatial relationship indicates that fabric A may have developed under the same extensional regime that produced the Blanice Graben and the last phase of brittle-ductile deformation.

Table 1

Laser ablation ICP-MS U-Pb data for zircon grains from the Benešov pluton (Bílkovice Quarry).

No.	Corrected isotope ratios					Apparent ages (Ma)				U, Th and Pb content (ppm)						Th/U
	$^{207}Pb/^{235}U$	±2s	$^{206}Pb/^{238}U$	±2s	error corr.	$^{207}Pb/^{235}U$	±2s	$^{206}Pb/^{238}U$	±2s	Approx U	±2s	Approx Th	±2s	Approx Pb	±2s	
1	0.3995	0.0058	0.0543	0.0007	0.6126	341	4.2	341	4.1	1070	20	866	11	456	6.2	0.8
2	0.4105	0.0088	0.0548	0.0009	0.5752	350	6.4	344	5.6	382	7	182	2.7	95	2	0.5
3	0.4119	0.0072	0.0561	0.0008	0.3891	351	5.1	352	4.9	632	13	271	4.3	142	2.5	0.4
4	0.4087	0.0080	0.0556	0.0009	0.5933	348	5.7	348	5.4	446	9	288	3.8	152	2.9	0.6
5	0.4040	0.0080	0.0548	0.0008	0.4859	345	5.8	344	5.1	689	12	486	6.7	255	4.3	0.7
6	0.4053	0.0083	0.0540	0.0009	0.5834	345	6.0	339	5.3	517	8.1	377	4.3	196	3.4	0.7
7	0.4004	0.0065	0.0542	0.0008	0.5435	342	4.6	340	4.8	1042	18	917	9.5	473	5.8	0.9
8	0.4084	0.0074	0.0549	0.0008	0.6022	348	5.2	344	4.8	659	13	505	7.3	260	4.1	0.8
9	0.4206	0.0081	0.0566	0.0009	0.5193	356	5.8	355	5.6	425	5.8	199	2.5	103	2.2	0.5
10	0.4133	0.0082	0.0556	0.0009	0.5663	352	5.8	349	5.7	508	10	368	6.9	193	4.6	0.7
11	0.4160	0.0073	0.0560	0.0009	0.4597	353	5.3	351	5.4	631	16	260	5.3	136	3.2	0.4
12	0.4110	0.0068	0.0551	0.0008	0.5262	349	4.9	346	4.9	794	11	569	6.5	300	4.4	0.7
13	0.4189	0.0069	0.0561	0.0008	0.4175	355	4.9	352	4.8	1221	26	785	18	442	13	0.6
14	0.4059	0.0087	0.0542	0.0010	0.5530	346	6.2	340	5.8	480	6.8	200	1.8	106	2	0.4
15	0.4023	0.0087	0.0542	0.0009	0.4572	343	6.4	340	5.6	419	8	201	3.2	106	2.4	0.5
16	0.4115	0.0080	0.0558	0.0009	0.3024	349	5.8	350	5.6	354	3.7	165	1.5	87	1.6	0.5
17	0.4113	0.0082	0.0553	0.0010	0.7084	349	5.9	348	6.4	594	11	286	3.6	155	3.2	0.5
18	0.4154	0.0098	0.0560	0.0008	0.3940	353	7.0	351	5.0	275	7.9	134	4.1	70	2.5	0.5
19	0.4007	0.0079	0.0544	0.0010	0.5575	342	5.7	342	6.0	534	8.6	256	3.2	136	2.3	0.5
20	0.4122	0.0061	0.0560	0.0009	0.5453	350	4.4	352	5.2	2631	32	754	12	381	8	0.3
21	0.4130	0.0067	0.0554	0.0010	0.5041	351	4.8	348	6.0	1254	46	538	18	280	11	0.4
22	0.3986	0.0088	0.0545	0.0010	0.5036	340	6.3	343	6.2	395	7.3	277	4.4	149	2.8	0.7
23	0.4076	0.0063	0.0548	0.0008	0.4910	347	4.6	344	5.1	1577	18	580	5.6	295	4.3	0.4
24	0.3993	0.0099	0.0542	0.0010	0.5613	342	7.2	341	6.2	352	7.6	264	6.3	141	4.2	0.7
25	0.4122	0.0081	0.0560	0.0009	0.6509	350	5.9	351	5.5	603	8.9	419	10	223	5.9	0.7
26	0.3995	0.0092	0.0541	0.0011	0.4721	341	6.6	340	6.8	423	12	188	3.3	103	2.4	0.4
27	0.4043	0.0092	0.0549	0.0012	0.5644	344	6.6	345	7.0	372	13	179	4.6	96	3.4	0.5
28	0.4103	0.0074	0.0554	0.0011	0.5173	349	5.3	348	6.5	1471	22	641	10	357	8.3	0.4
29	0.4086	0.0068	0.0553	0.0007	0.5506	347	4.9	347	4.4	1071	17	827	8.6	451	6.3	0.8
30	0.4055	0.0059	0.0549	0.0008	0.6301	346	4.2	345	4.9	1604	26	1078	24	608	14	0.7
31	0.4136	0.0084	0.0549	0.0010	0.5650	352	6.0	345	5.9	809	30	552	28	314	16	0.7
32	0.4205	0.0081	0.0560	0.0010	0.5073	356	5.8	351	5.9	507	12	374	13	208	7.1	0.7
33	0.4115	0.0086	0.0550	0.0010	0.5301	351	6.1	345	5.8	426.8	7.9	209	3.4	111.7	2.5	0.5

(B) The second group of AMS fabric (fabric B_{mag}) represents the dominant foliation dipping NW and the lineation plunging gently NNW. It also was recognized at a mesoscopic scale (fabric B_{meso}). Brittle deformation of plagioclase (see Fig. 5C–F) indicates temperatures lower than approx. 400 °C (Suppe, 1985), while ductile deformation of aplitic dikes (Fig. 4A–C) requires temperatures higher than approximately 300 °C (Suppe, 1985). These constraints are in accordance with chlorite and muscovite crystallization in shear zones (Fig. 5D–F). Thus, this fabric originated under temperature conditions characterising moderate cooling of the Benešov intrusion. Fabric B is associated with a top-to-the-NW shearing (Figs 4E, 5F), associated with low-angle normal displacements (Figs 3, 7). This deformation may have led to tectonic unroofing of the Benešov pluton. Furthermore, it may have enhanced subsidence of Pennsylvanian sedimentary basins that are located W and N of the study area (Fig. 1B). The initiation of the Intra-Sudetic Basin southeast of the Karkonosze pluton (Mazur 1995; Mazur and Aleksandrowski, 2001) may serve as an analogue within the Bohemian Massif. Putting all this together, normal shearing- and faulting-related fabric B probably was connected with the main extensional event leading to unroofing of the central parts of the Bohemian Massif.

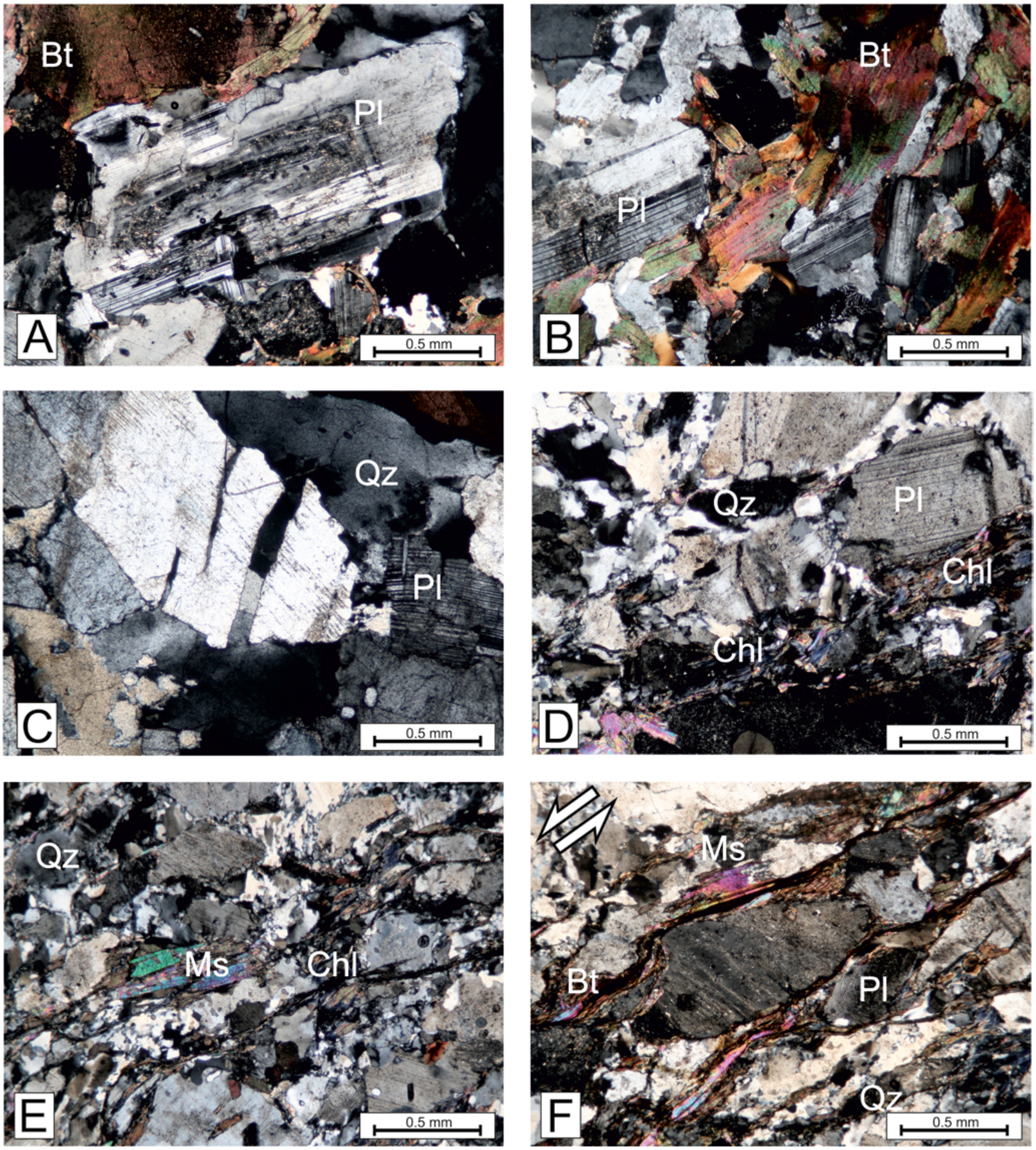

Fig. 5. Photomicrographs of the Benešov granodiorite (cross-polarized light). **A.** Oscillatory zoning in plagioclase partly overprinted by mechanical flame-shaped twins, Střížkov. **B.** Low degree of anisotropy, plagioclase with both magmatic and mechanical twinning; Střížkov. **C.** plagioclase grain with brittle fractures filled with remobilized quartz, Sembrantec. **D.** lobate quartz grains with undulatory extinction and newly formed chlorite, Vestec. **E.** recrystallized quartz grains and newly formed muscovite and chlorite, Vestec. **F.** S-C structure with a σ-type porphyroclast, Vestec. Explanations: Qz – quartz, Pl – plagioclase, Bi – biotite, Chl – chlorite, Ms – muscovite.

(C) The last group of AMS fabrics (fabric C_{mag}) is more enigmatic and occurs only locally. These structures, preserved in AMS only, are characterised by the smallest degree of anisotropy *P*. This indicates a small degree of preferred orientation (Fig. 7) and, consequently, a modest rock deformation. Inhomogeneous, weak deformation also could have contributed to its directional dispersion. The microstructures studied (Fig. 5A, B), such as mechanical twinning of plagioclase, slightly bent biotite flakes, and quartz grains with more-or-less continuous undulatory extinction, indicating dislocation glide and the possible initial stage of recovery, manifest low-strain damage of the original

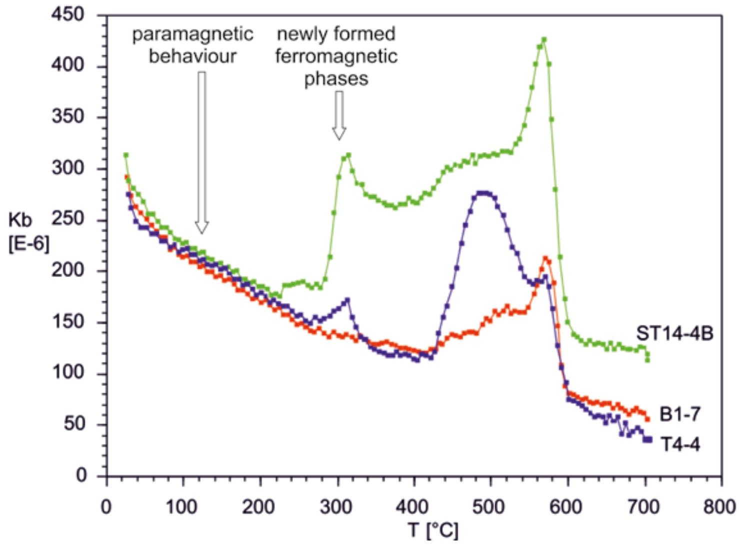

Fig. 6. Thermomagnetic measurements of the Benešov granodiorite from three representative sites (T4-4 – Třebešice, ST14-4B – Střížkov, B1-7 – Bílkovice) showing a hyperbolical decrease in bulk susceptibility at the beginning, typical of paramagnetic minerals, and newly formed ferromagnetic phases under high-temperature conditions.

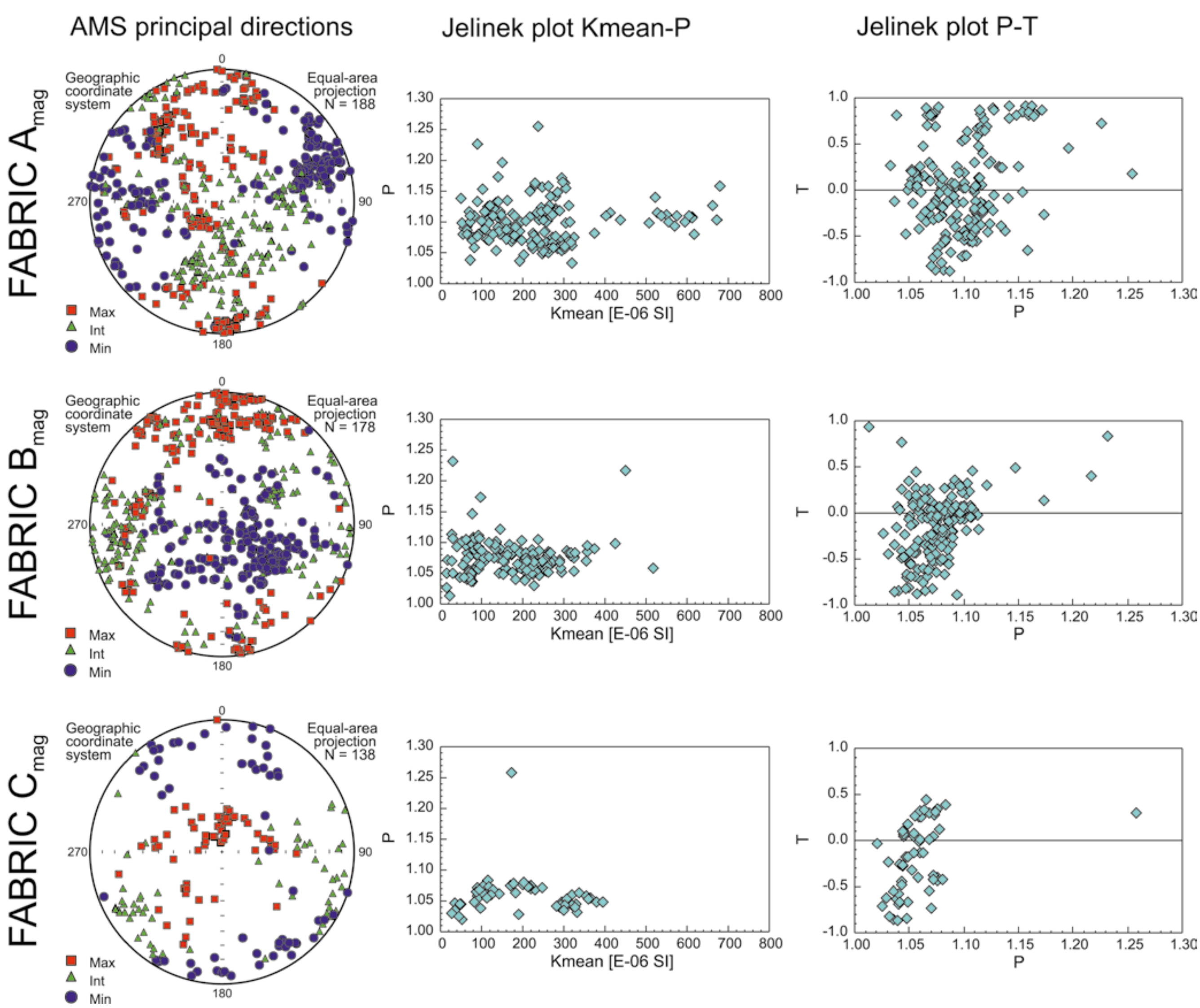

Fig. 7. Three types of recognized AMS fabrics and their characteristics.

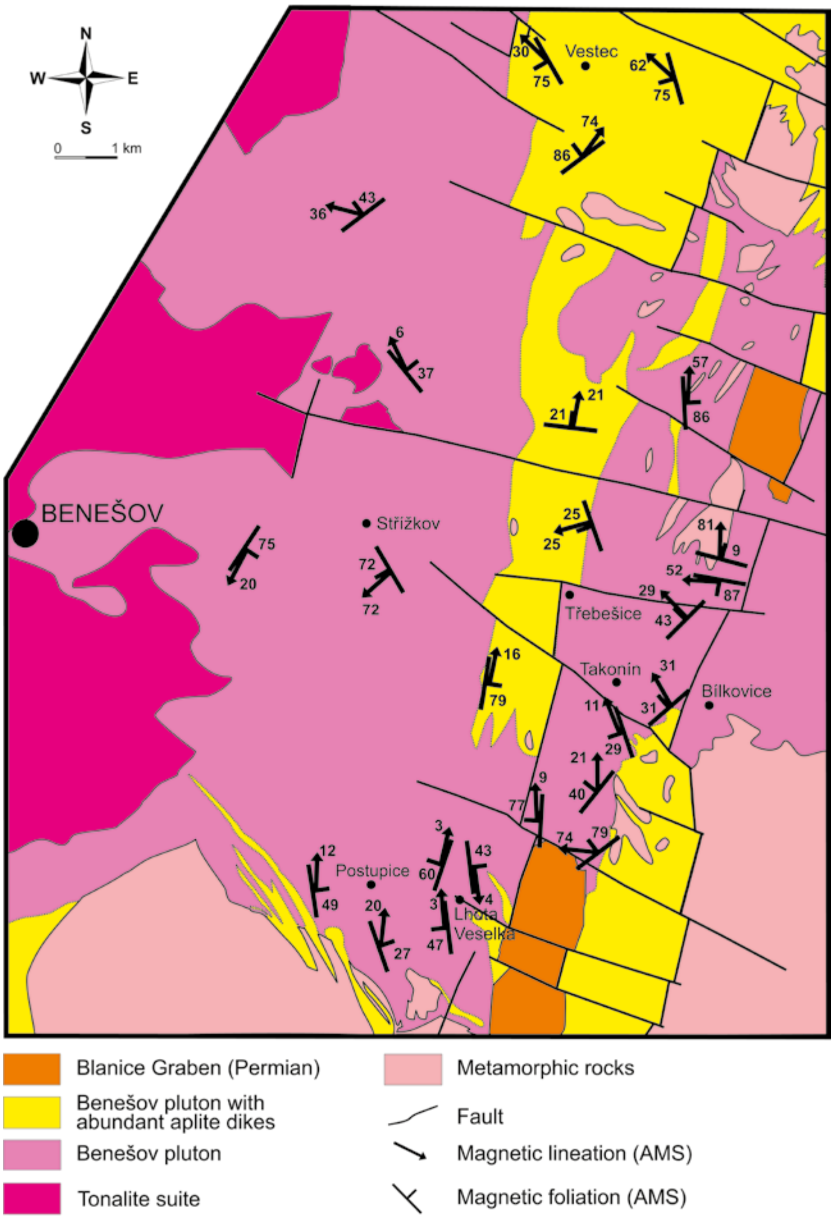

Fig. 8. Simplified geological map of the Benešov pluton with magnetic foliations and lineations indicated.

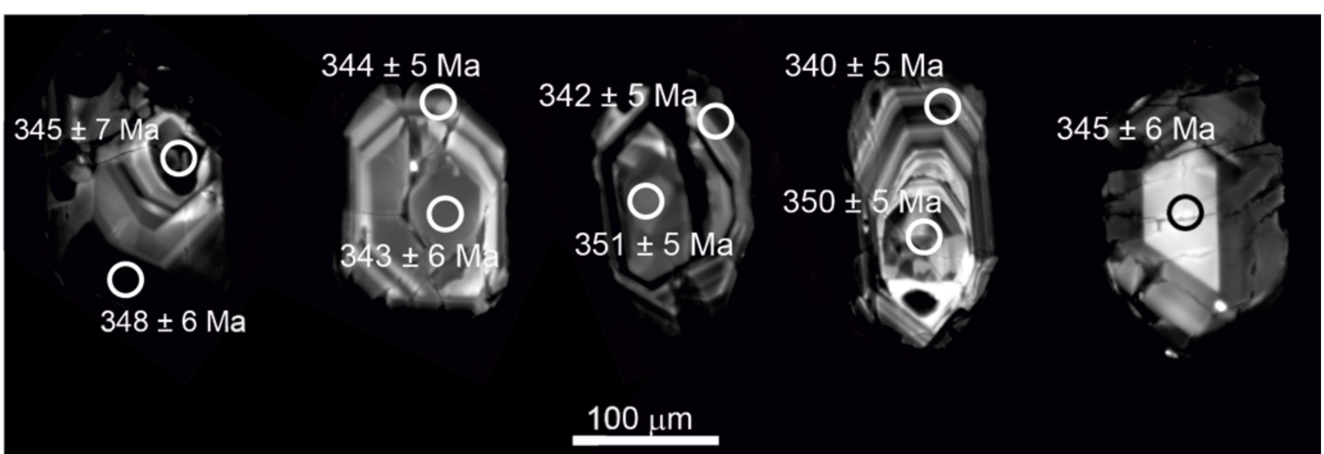

Fig. 9. Radiometric ages of zircon grains from the Benešov pluton: oscillatory-zoned zircon grains in cathodoluminescence imaging, Bílkovice Quarry.

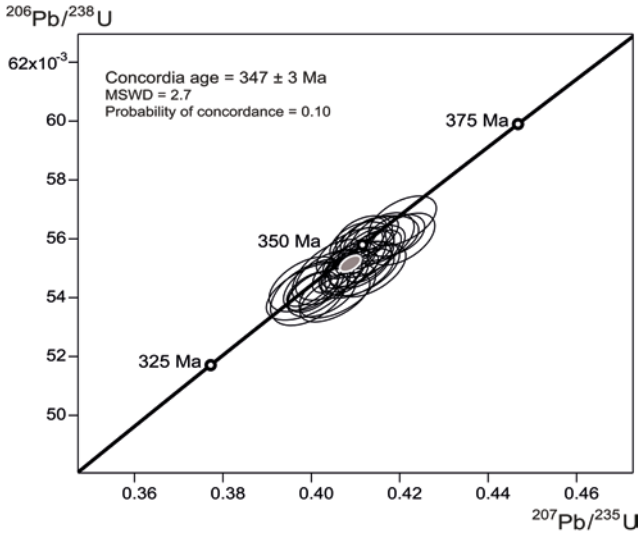

Fig. 10. U–Pb Concordia diagram for zircon grains from the Benešov pluton, Bílkovice Quarry.

magmatic fabric. The strike of the magnetic foliation is mostly NE–SW (Fig. 7), which is similar to the strike of the Central Bohemian shear zone and the elongation of the CBPC (Fig. 1). Although with low anisotropy and, consequently, high dispersion, the orientation of C_{mag} reflects the shape of the pluton. Therefore, the authors interpret C_{mag} as the oldest fabric. It might be a relic fabric that is connected with the emplacement of the Benešov pluton. The age related to this fabric, can be therefore considered relatively close to the magmatic age (347±3 Ma).

Directionally different fabrics, both magnetic and mesoscopic, are products of sequential events during the late Variscan evolution and can be attributed to a few extensional events. Figure 11 shows the possible timing for the development of three fabrics, recognised in the Benešov pluton, and their relationship to the regional magmatic and sedimentary events in the central part of the Bohemian Massif.

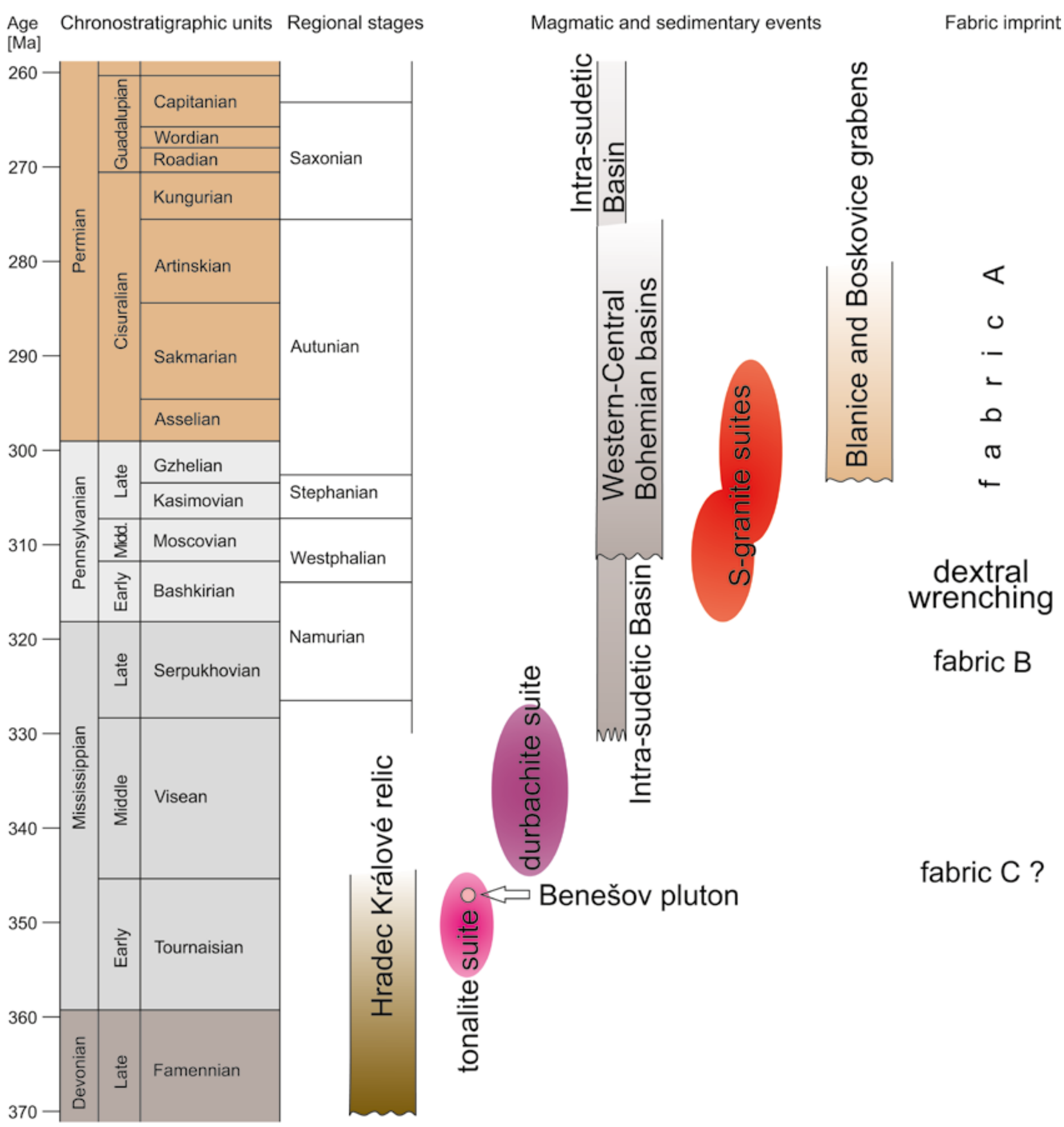

Fig. 11. Scheme of the main magmatic and sedimentary events in the central part of the Bohemian Massif and their timing. Tectonic events documented in the Benešov pluton are included.

Age of the dominant phase of extension (fabric B)

The age related to fabric B (B_{meso} and B_{mag}) must be younger than the magmatic age of the Benešov pluton. The herein described brittle-ductile, normal dip-slip shearing to the NW and N along foliation planes in the Benešov pluton has been also recognized in other localities at the border zone of the Bohemicum and Moldanubicum units, such as the CBPC (Žák *et al*., 2012), Železné hory plutonic complex (Pitra *et al*., 1994) including the Miřetín pluton (Verner and Vondrovic, 2010; Vondrovic *et al*., 2011), and durbachite bodies (Mlynář and Melichar, 1999). As similar deformation affected the durbachite intrusion, dated at 343–332 Ma in age (Klomínský *et al*., 2010), the authors consider this age as a maximum limit for the formation of the B-fabric.

Since the Benešov granodiorite is overlain by latest Carboniferous to Permian (Gzhelian–Cisuralian, i.e., ~303–280 Ma) sedimentary rocks, it must have been exposed at the surface at that time. As the heterogeneous, wide zone of shearing associated with fabric B is displaced along dextral strike-slip shear zones, together with other structures (Fig. 1B), the time of dextral wrenching in the Variscan orogen (Edel *et al*., 2018) can be considered as a minimum age limit for the origin of fabric B (~325–310 Ma).

Taking these constraints into account, the beginning of the gravitational collapse in the central part of the Bohemian Massif can be assigned to the late Viséan (~332 Ma), which is in accordance with the extensional initiation of the Intra-Sudetic Basin (Mazur 1995; Mazur and Kryza, 1996; Turnau *et al*., 2002), and the main movements continued into the Serpukhovian. Considering the kinematics of shear zones, the most probable interpretation is that the tectonic regime represented by fabric B controlled the formation of the Western and Central Bohemian basins (Moscovian–late Cisuralian).

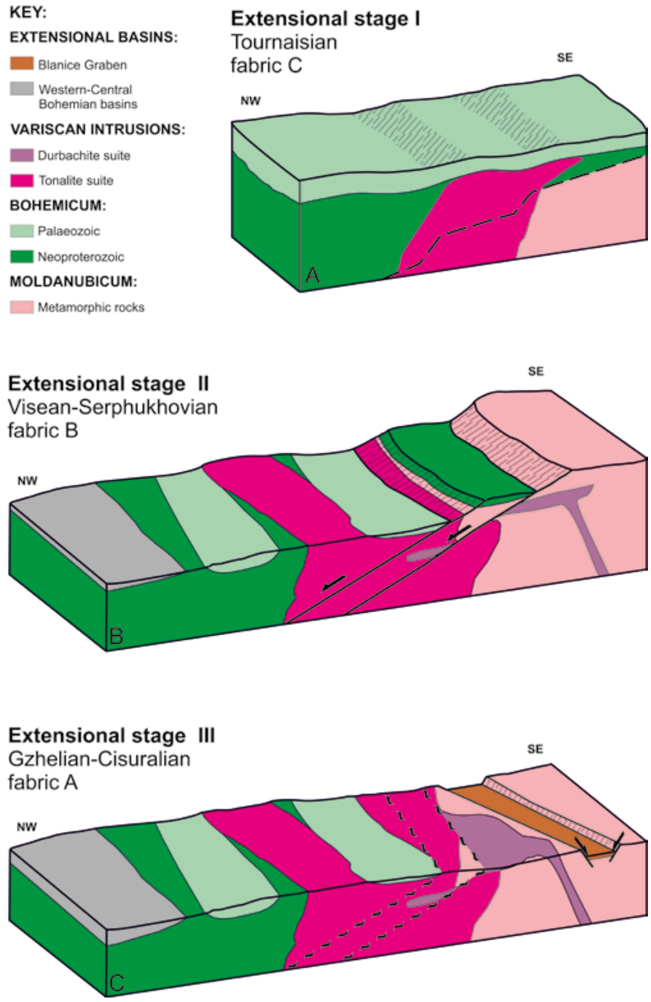

Fig. 12. An evolutionary model of the Variscan orogen in Central Bohemia. Three extensional phases are well evidenced near the Bohemicum/Moldanubicum boundary.

CONCLUSIONS – A MODEL OF LATE-VARISCAN TECTONIC EVOLUTION

The recognition of three different fabric types in the Benešov pluton and their age constraints allows reconstruction of the possible extensional history during three stages of gravitational collapse. During extensional stage I, the Benešov granodiorite was emplaced at 347±3 Ma (Fig. 12A) and Fabric C was formed. The extensional stage of plutonism was followed by normal dip-slip shearing of extensional stage II, mainly during the late Mississippian (late Viséan to Serpukhovian, i.e., ~332–320 Ma). During this stage, the dominant B-fabric with normal shearing to NW–N originated and the main unroofing took place, controlling the origin of an elongated depression, later filled with Moscovian sediments (Fig. 12B). The last extensional stage III occurred in the period of the latest Pennsylvanian (Gzhelian) to Permian (Cisuralian), i.e., at ~303–280 Ma, when brittle-ductile fabric A striking NNW-SSE to NNE-SSW was formed. This last stage was connected with the origin of Permo–Carboniferous troughs in the Bohemian Massif (Fig. 12C).

Acknowledgments

The authors thank Alice Zavřelová for her help with the hand-picking of zircon grains and to Martin Svojtka for radiometric dating at the Institute of Geology of the CAS in Prague. A big thank you to AGICO, Inc., for providing their magnetometric facilities, especially to Martin Chadima for conducting cryometry. J. Černý acknowledges the Czech Science Foundation (GACR; Grant Project 19–02177Y) and the institutional support provided by the Institute of Geology, Czech Academy of Sciences, assigned to RVO: 67985831.

REFERENCES

Borradaile, J. G. & Henry, B., 1997. Tectonic applications of magnetic susceptibility and its anisotropy. *Earth-Science Reviews*, 42: 49–93.

Bouchez, J-L., 1997. Granite is never isotropic: An introduction to AMS studies in granitic rocks. In: Bouchez, J. L., Hutton, D. H. W. & Stephens, W. E. (eds), *Granite: from Segregation of Melt to Emplacement Fabrics*. Kluwer Academic, Dordrecht, pp. 95–112.

Bouchez, J-L., 2000. Anisotropie de susceptibilité magnétique et fabrique des granites. *Comptes Rendus de l'Académie* *des Sciences, Series IIA, Earth and Planetary Science*, 330: 1–14.

Bouchez, J-L., Gleizes, G., Djouadi, T. & Rochette, P., 1990. Microstructure and magnetic susceptibility applied to emplacement kinematics of granites: The example of the Foix pluton (French Pyrenees). *Tectonophysics*, 184: 157–171.

Čech, V., Havlíček, V. & Zikmundová, J., 1989. The Upper Devonian and Lower Carboniferous in northeastern Bohemia (based on boreholes in the Hradec Králové area). *Věstník Ústředního ústavu geologického*, 64: 65–75.

Chadima, M. & Jelínek, V., 2008. Anisoft 4.2 – anisotropy data browser. *Contributions to Geophysics and Geodesy*, 38 (Special Issue), p. 41.

Chlupáč, I. & Zikmundová, J., 1976. The Devonian and Lower Carboniferous in the Nepasice bore in East Bohemia. *Věstník Ústředního ústavu geologického*, 51: 269–278.

Dragoun, F., Holub, F., Chlupáčová, M., Kachlík, V., Verner, K. & Žák, J., 2009. Forearc deformation and strain partitioning during growth of a continental magmatic arc: The northwestern margin of the Central Bohemian Plutonic Complex, Bohemian Massif. *Tectonophysics*, 469: 93–111.

Edel, J. B., Schulmann, K., Lexa, O. & Lardeaux, J. M., 2018. Late Palaeozoic palaeomagnetic and tectonic constraints for amalgamation of Pangea supercontinent in the European Variscan belt. *Earth-Science Reviews*, 177: 589–612.

Falke, H. (ed.), 1975. *The Continental Permian in Central, West, and South Europe. Proceedings of the NATO Advanced Study Institute held at the Johannes Gutenberg University, Mainz, F.R.G., 23 September – 4 October, 1975*. D. Reidel Publishing Company, Dordrecht, Holland / Boston, U.S.A., 352 pp.

Franke, W., 1992. Phanerozoic structures and events in Central Europe. In: Blundel, D., Freeman, R. & Mueller, S. (eds), *A Continent Revealed. The European Geotraverse*. Cambridge University Press, Cambridge, pp. 160–180.

Franke, W., 2000. The mid-European segment of the Variscides: tectonostratigraphic units, terrane boundaries and plate tectonic evolution. In: Franke, W., Haak, V., Oncken, O. & Tanner, D. (eds), *Orogenic Processes: Quantification and Modelling in the Variscan Belt. Geological Society, London, Special Publications*, 179: 35–61.

Graham, J. W., 1954. Magnetic susceptibility anisotropy, an unexploited petrofabric element. *Geological Society of America Bulletin*, 65: 1257–1258.

Henk, A., 1996. Gravitational orogenic collapse vs plate-boundary stresses: a numerical modelling approach to the Permo-Carboniferous evolution of Central Europe. *Geologische Rundschau*, 86: 39–55.

Holub, F., Cocherie, A. & Rossi, P., 1997a. Radiometric dating of granitic rocks from the Central Bohemian Plutonic Complex (Czech Republic): constraints on the chronology of thermal and tectonic events along the Moldanubian–Barrandian boundary. *Comptes Rendus de l'Académie des Sciences, Series IIA, Earth and Planetary Science*, 325: 19–26.

Holub, F. V., Machart, J. & Manová, M., 1997b. The Central Bohemian Plutonic Complex: geology, chemical composition and genetic interpretation. *Sborník geologických věd, Ložisková geologie*, 31: 27–50.

Hoskin, P. W. O. & Schaltegger, U., 2003. The composition of zircon and igneous and metamorphic petrogenesis. *Reviews in Mineralogy and Geochemistry*, 53: 27–62.

Hrouda, F., 1994. A technique for the measurement of thermal changes of magnetic susceptibility of weakly magnetic rocks by the CS-2 apparatus and KLY-2 Kappabridge. *Geophysical Journal International*, 118: 604–612.

Hrouda, F., 1999. Magnetic fabric in granitic rocks: its intrusive origin and post-intrusive tectonic modification. *Geolines*, 8: 29.

Jackson, S. E., Pearson, N. J., Griffin, W. L. & Belousova, E. A., 2004. The application of laser ablation-inductively coupled plasma-mass spectrometry to in situ U-Pb zircon geochronology. *Chemical Geology*, 211: 47–69.

Jadamec, M. A., Turcotte, D. L. & Howell, P., 2007. Analytic models for orogenic collapse. *Tectonophysics*, 435: 1–12.

Janoušek, V., Bowes, D., Rogers, G., Farrow, C. M. & Jelínek, E., 2000. Modelling diverse processes in the petrogenesis of a composite batholith: the Central Bohemian Pluton, Central European Hercynides. *Journal of Petrology*, 41: 511–543.

Janoušek, V. & Gerdes, A., 2003. Timing the magmatic activity within the Central Bohemian Pluton, Czech Republic: Conventional U-Pb ages for the Sázava and Tábor intrusions and their geotectonic significance. *Journal of the Czech Geological Society*, 48: 70–71.

Jelínek, V., 1981. Characterization of the magmatic fabric of rocks. *Tectonophysics*, 79: T63–T67.

Jelínek, V. & Pokorný, J., 1997. Some new concepts in technology of transformer bridges for measuring susceptibility anisotropy of rocks. *Physics and Chemistry of the Earth*, 22: 179–181.

Jokubauskas, P., Bagiński, B., Macdonald, R. & Krzemińska, E., 2018. Multiphase magmatic activity in the Variscan Kłodzko–Złoty Stok intrusion, Polish Sudetes: evidence from SHRIMP U–Pb zircon ages. *International Journal of Earth Sciences*, 107: 1623–1639.

Klomínský, J., Jarchovský, T. & Rajpoot, G., 2010. *Atlas of Plutonic Rocks and Orthogneisses in the Bohemian Massif.* Czech Geological Survey, Praha, 613 pp.

Koutek, J. & Urban, K., 1929. Note sur terrain granitique à l'Est de Benešov dans la Bohême centrale. *Věstník Státního geologického ústavu Československé republiky*, 15: 131–137. [In Czech, with French summary.]

Kroner, U. & Romer, R. L., 2013. Two plates – Many subduction zones: The Variscan orogeny reconsidered. *Gondwana Research*, 24: 298–329.

Kylander-Clark, A. R. C., Hacker, B. R. & Cottle, J. M., 2013. Laser-ablation split-stream ICP petrochronology. *Chemical Geology*, 345: 99–112.

Lobkowicz, M., Štědrá, V. & Schulmann, K., 1996. Late-Variscan extensional collapse of the thickened Moldanubian crust in the southern Bohemia. *Journal of the Czech Geological Society*, 41: 123–38.

Malavieille, J., 1993. Late Orogenic Extension in Mountains Belts: Insight from the Basin and Range and the Late Paleozoic Variscan Belt. *Tectonics*, 12: 1115–1130.

Malavieille, J., Guihot, P., Costa, S., Lardeaux, J. M. & Gardien, V., 1990. Collapse of the thickened Variscan crust in the French Massif Central: Mont Pilat extensional shear zone and St. Etienne Late Carboniferous basin. *Tectonophysics*, 117: 139–149.

Matte, P., 1991. Accretionary history and crustal evolution of the Variscan belt in Western Europe. *Tectonophysics*, 196: 309–337.

Matte, P., 2001. The Variscan collage and orogeny (480–290 Ma) and the tectonic definition of the Armorica microplate: a review. *Terra Nova*, 13: 122–128.

Mazur, S., 1995. Structural and metamorphic evolution of the country rocks at the eastern contact of the Karkonosze granite in the southern Rudawy Janowickie Mts and Lasocki Range. *Geologia Sudetica*, 29: 31–98. [In Polish, with English summary.]

Mazur, S. & Aleksandrowski, P., 2001. The Teplá(?)/Saxothuringian suture in the Karkonosze-Izera massif, Western Sudetes, Central European Variscides. *International Journal of Earth Science*s, 90: 341–360.

Mazur, S. & Kryza, R., 1996. Superimposed compressional and extensional tectonics in the Karkonosze-Izera Block, NE Bohemian Massif. In: Oncken, O. & Janssen, C. (eds), *Basement Tectonics 11*. Springer, Dordrecht, pp. 51–66.

Melichar, R., 2004. Tectonics of the Prague Synform: a hundred years of scientific discussion. *Krystalinikum*, 30: 167–187.

Mikulski, S. Z., Williams, I. S. & Bagiński, B., 2013. Early Carboniferous (Viséan) emplacement of the collisional Kłodzko–Złoty Stok granitoids (Sudetes, SW Poland): constraints from geochemical data and zircon U-Pb ages. *International Journal of Earth Sciences*, 102: 1007–1027.

Mlynář, A. & Melichar, R., 1999. Tectonically strained durbachites from the vicinity of Nové Město na Moravě (Western Moravia). *Geologické výzkumy na Moravě a ve Slezsku*, 6: 114–116. [In Czech, with English summary.]

Nagata, T., 1961. *Rock Magnetism, Second Edition*. Maruzen Company Ltd., Tokyo, 350 pp.

Orlov, A., 1933. Contribution à l'étude pétrographique du massif „granitique“ de la Bohême Centrale (région de Říčany-Benešov-Milevsko-Písek). *Věstník Státního geologického Ústavu Československé Republiky*, 9: 135–144. [In Czech, with French summary.]

Paton, C., Hellstrom, J., Paul, B., Woodhead, J. & Hergt, J., 2011. Iolite: Freeware for the visualisation and processing of mass spectrometric data. *Journal of Analytical Atomic Spectrometry*, 26: 2508–2518.

Pešek, J., 1994. *Carboniferous of Central and Western Bohemia*. Czech Geological Survey, Prague, 60 pp.

Petrus, J. A. & Kamber, B. S., 2012. VizualAge: A novel approach to laser ablation ICP-MS U-Pb geochronology data reduction. *Geostandards and Geoanalytical Research*, 36: 247–270.

Pitra, P., Burg, J. P., Schulmann, K. & Ledru, P., 1994. Late orogenic extension in the Bohemian Massif: petrostructural evidence in the Hlinsko region. *Acta Geodynamica*, 7: 15–30.

Porębski, S. J., 1981. Świebodzice succession (upper Devonian-lowest Carboniferous; Western Sudetes): a prograding, mass-flow dominated fan-delta complex. *Geologia Sudetica*, 16: 101–192. [In Polish, with English summary.]

Porębski, S. J., 1990. Onset of coarse clastic sedimentation in the Variscan realm of the Sudetes (SW Poland): an example from the Upper Devonian-Lower Carboniferous Świebodzice succession. *Neues Jahrbuch für Geologie und Paläontologie, Abhandlungen*, 179: 259–274.

Pystina Y. & Pystin, A., 2019. Th/U relations as an indicator of the genesis of metamorphic zircons (on the example of the north of the Urals). In: Glagolev, S. (ed.), *14th International Congress for Applied Mineralogy (ICAM2019). Belgorod State Technological University named after V. G. Shukhov, 23–27 September 2019, Belgorod, Russia*. Springer Open, Cham, pp. 129–132.

Rey, P., Vanderhaeghe, O. & Teyssier, C., 2001. Gravitational collapse of the continental crust: definition, regimes and modes. *Tectonophysics*, 342: 435–449.

Rodríguez-Méndez, L., Cuevas, J. & Tubí, J. M., 2016. Post-Variscan basin evolution in the central Pyrenees: Insights from the Stephanian–Permian Anayet Basin. *Comptes Rendus Geoscience*, 348: 333–341.

Schaltegger, U., Schmitt, A. K. & Horstwood, S. A., 2015. U–Th–Pb zircon geochronology by ID-TIMS, SIMS, and laser ablation ICP-MS: Recipes, interpretations, and opportunities. *Chemical Geology*, 402: 89–110.

Schulmann, K., Konopásek, J., Janoušek, V., Lexa, O., Lardeaux, J. M., Edel, J. B., Štípská, P. & Ulrich, S., 2009. An Andean type Palaeozoic convergence in the Bohemian Massif. *Comptes Rendus Geoscience*, 341: 266–286.

Shore, M. & Fowler, A. D., 1996. Oscillatory zoning in minerals: a common phenomenon. *The Canadian Mineralogist*, 34: 1111–1126.

Sláma, J., Košler, J., Condon, D. J., Crowley, J. L., Gerdes, A., Hanchar, J. M., Horstwood, M. S. A., Morris, G. A., Nasdala, L., Norberg, N., Schaltegger, U., Schoene, B., Tubrett, M. N. & Whitehouse, M. J., 2008. Plešovice zircon: A new natural reference material for U-Pb and Hf isotopic microanalysis. *Chemical Geology*, 249: 1–35.

Stampfli, G. M., von Raumer, J. F. & Borel, G. D., 2002. Paleozoic evolution of pre-Variscan terranes: from Gondwana to the Variscan collision. In: Catalan, J. R. M., Hatcher, R. D., Arenas, R. & Garcia, F. D. (eds), *Variscan-Appalachian Dynamics: The Building of the Late Paleozoic Basement*, *Geological Society of America Special Papers*, 364: 263–280.

Suppe, J., 1985. *Principles of Structural Geology*. Prentice Hall, Englewood Cliffs, New Jersey, 537 pp.

Svoboda, J. (ed.), 1964. *Regionání geologie* ČSSR. *Díl, I, Český masív. Svazek 1, Krystalinikum.* Nakladatelstvví Československé akademie věd, Praha, 378 pp. [In Czech.]

Tarling, D. H. & Hrouda, F., 1993. *The Magnetic Anisotropy of Rocks*. Chapman and Hall, London, 217 pp.

Tunheng, A. & Hirata, T., 2004. Development of signal smoothing device for precise elemental analysis using laser ablation-ICP-mass spectrometry. *Journal of Analytical Atomic Spectrometry*, 19: 932–934.

Turnau, E., Żelaźniewicz, A. & Franke, W., 2002. Middle to early late Viséan onset of late orogenic sedimentation in the Intra-Sudetic Basin, West Sudetes: miospore evidence and tectonic. *Geologia Sudetica*, 34: 9–16.

Vejnar, Z., 1974. Application of cluster analysis in the multivariate petrochemical classification of the rocks of the Central Bohemian Pluton. *Věstník Ústředního ústavu geologického*, 49: 29–34. [In Czech, with English summary.]

Verner, K. & Vondrovic, L., 2010. The record of structural evolution and U-Pb zircon dating of the tonalite intrusions (Policka Crystalline Unit, Bohemian Massif). *Trabajos de Geología*, 30: 316–321.

Vondrovic, L., Verner, K., Buriánek, D., Halodová, P., Kachlík, V. & Míková, J., 2011. Emplacement, structural and P–T evolution of the ~346 Ma Miřetín Pluton (eastern Teplá-Barrandian Zone, Bohemian Massif): implications for regional transpressional tectonics. *Journal of Geoscience*, 56: 343–357.

Weidenbeck, M., Allé, P., Corfu, F., Griffin, W. L., Meier, M., Oberli, F., von Quadt, A., Roddick, J. C. & Spiegel, W., 1995. Three natural zircon standards for U-Th-Pb, Lu-Hf, trace element and REE analyses. *Geostandards Newsletter*, 19: 1–23.

Žák, J., Sláma, J. & Burjak, M., 2017. Rapid extensional unroofing of a granite-migmatite dome with relics of high-pressure rocks, the Podolsko complex, Bohemian Massif. *Geological Magazine*, 154: 354–380.

Žák, J., Verner, K., Holub, V. F., Kabele, P., Chlupáčová, M. & Halodová, P., 2012. Magmatic to solid state fabrics in syntectonic granitoids recording early Carboniferous orogenic collapse in the Bohemian Massif. *Journal of Structural Geology*, 36: 27–42.